$^{12}C(^{12}C,\alpha)^{20}Ne$ excitation functions and angular distributions*

L. R. Greenwood, R. E. Segel, K. Raghunathan, and M. A. Lee
Northwestern University, Evanston, Illinois 60201
and Argonne National Laboratory, Argonne, Illinois 60439

H. T. Fortune
Argonne National Laboratory, Argonne, Illinois 60439
and University of Pennsylvania, Philadelphia, Pennsylvania 19104

J. R. Erskine
Argonne National Laboratory, Argonne, Illinois 60439
(Received 13 March 1975)

Excitation functions have been measured at a laboratory angle of 5° over an incident energy range of 18–25.5 MeV (c.m.) for the $^{12}C(^{12}C,\alpha)$ reaction leading to about 30 levels in ^{20}Ne (E_x = 0–20 MeV). Angular distributions were measured at five energies. An Ericson fluctuation analysis yields the result that most levels are populated by a large nonstatistical reaction component. A significant compound-nuclear component is also present, with correlation widths on the order of 150–250 keV (c.m.). The energy-averaged cross sections have been compared with statistical compound-nuclear (Hauser-Feshbach) calculations. This comparison indicates the presence of a strong direct-reaction mechanism, especially for the members of the proposed 8p-4h band (at 7.196, 7.834, 9.040, and 12.16 MeV). A pronounced minimum in the excitation functions is evident at $E_{c.m.}$ = 19.2 MeV, near the recently reported strong resonance in the $^{12}C(^{12}C,p)^{23}Na$ channel. Other correlated effects also appear to be present at specific energies, but the cross correlations, calculated for the entire energy range, are largely statistical.

[NUCLEAR REACTIONS $^{12}C(^{12}C,\alpha)$, 5° yield curves $E_{^{12}C}$ 36–51 MeV, angular distribution 37, 41, 45, 48, and 51 MeV, statistical analyses.]

I. INTRODUCTION

The mechanism of heavy-ion reactions in which many nucleons are transferred is of interest since the observation of a direct component affords the opportunity to study specific clusters in nuclear states. Early studies of the $^{12}C(^{12}C,\alpha)^{20}Ne$ reaction,[1,2] as well as similar studies for $^{12}C(^{16}O,\alpha)^{24}Mg$[3,4] have shown that these reactions proceed predominantly by a statistical compound-nuclear process. However, the early investigations of the present reaction were carried out at rather low incident energies, $E_{c.m.}$=9–16 MeV, and examined the behavior of only a few low-lying states in ^{20}Ne.

Two recent studies of $^{12}C+^{12}C$ at higher incident energies have found strong evidence for nonstatistical reaction processes. In the $^{12}C(^{12}C,\alpha)$ reaction for a large range of incident energies ($E_{c.m.}$ = 11–17.5 MeV), Middleton, Garrett, and Fortune[5] observed the selective population of a $J^\pi=2^+$ level at 7.834 MeV in ^{20}Ne with an average cross section about five times that of a nearby 2^+ level at 7.424 MeV. In agreement with theoretical calculations,[6] Middleton *et al.* proposed that the 7.834-MeV level is part of a $K^\pi=0^+$ band whose dominant configuration is two α particles outside of a ^{12}C core. The selective population of states in this band would then be easily explained by the direct transfer of either a ^8Be or 2-α cluster. Van Bibber *et al.*[7] have recently observed a strong correlated resonance near $E_{c.m.}$ = 19.3 MeV in the $^{12}C(^{12}C,p)$ reaction to several levels above 9 MeV in ^{23}Na, thus also suggesting the presence of a nonstatistical process.

In the present work we have measured excitation functions and angular distributions for about 30 levels up to about 20 MeV excitation in ^{20}Ne. The observed relative populations of various states have been used to gain further insight into the reaction mechanism and the band structure of ^{20}Ne. The data have also been analyzed as Ericson fluctuations and the average cross sections have been compared to detailed statistical Hauser-Feshbach compound-nuclear calculations.

II. EXPERIMENTAL PROCEDURE

Excitation functions at 5°(lab) were measured for α particles leading to final states in ^{20}Ne, $E_x \leq 20$ MeV, in steps of 125 keV(lab) over the range of incident energies E_{lab} = 36–51 MeV using the ^{12}C beam from the Argonne FN tandem accelerator. Self-supporting ^{12}C targets of ~10-μg/cm^2 thickness were surrounded by a LN_2 cold sleeve

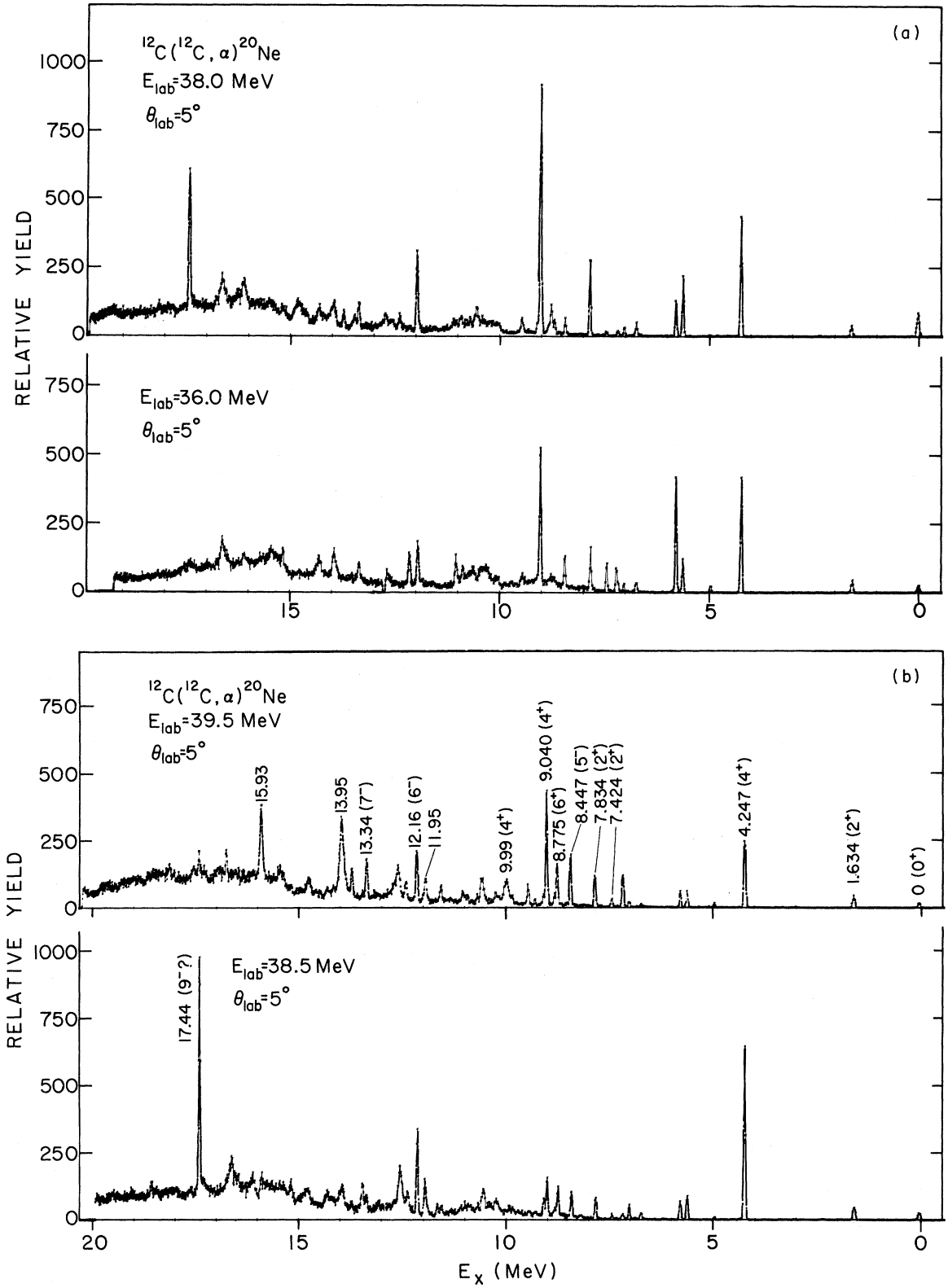

FIG. 1. Spectra for the $^{12}C(^{12}C, \alpha)^{20}Ne$ reaction at $\theta_{lab} = 5°$ at $E_{lab}(^{12}C) =$: (a) 36.0 and 38.0 MeV, (b) 38.5 and 39.5 MeV, and (c) 40.0 and 42.0 MeV. Note the large fluctuations for individual levels from energy to energy.

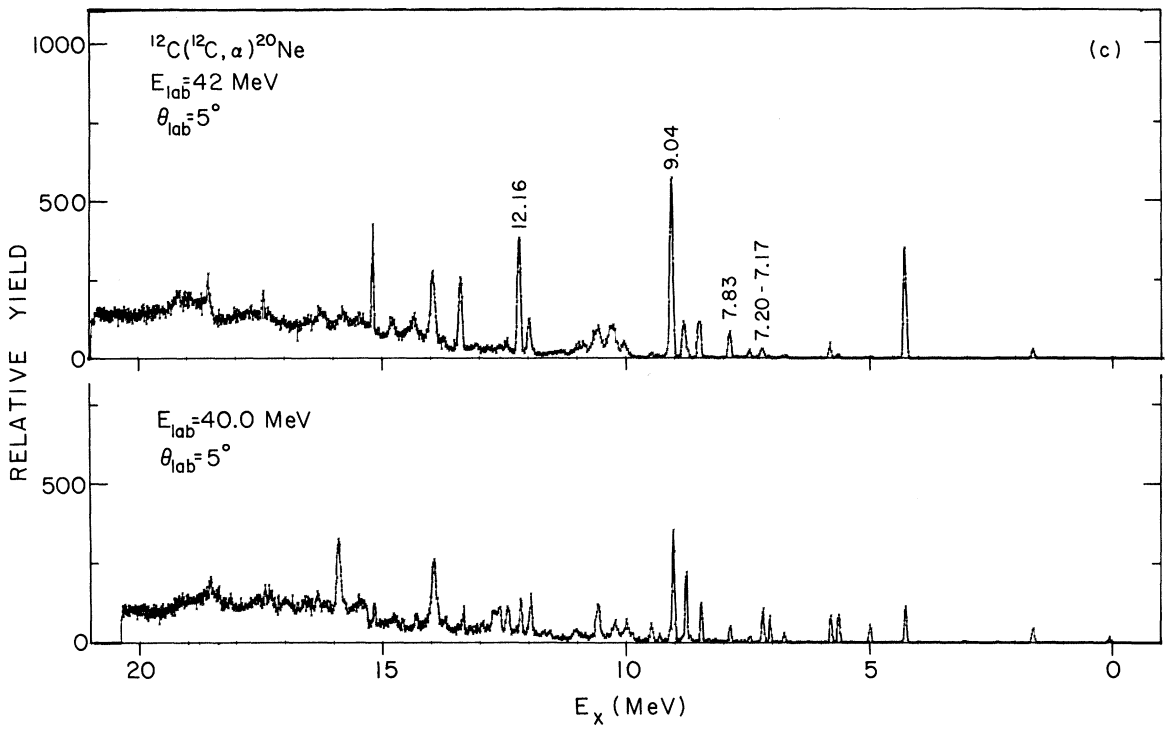

FIG. 1 *(Continued)*

to minimize carbon buildup. The buildup was measured to be less than 0.5 $\mu g/cm^2$ per mC of beam particles.

The α particles were detected with a 50-cm-long position-sensitive proportional counter[8] placed in the focal plane of a split-pole magnetic spectrograph. A solid angle of 1 msr was used. This combination made the experiment feasible since it afforded us both high resolution and rapid data acquisition. Furthermore, it was possible to display and analyze the data on line, thus providing a ready check on the quality of the measured spectra during its acquisition. Were the counter not available, it would have been necessary to use plates and the measurement of more than four hundred exposures would have required an inordinate amount of changing, developing, and scanning of nuclear emulsions.

Since the counter length (50 cm) allowed us to observe only a limited region of excitation energies, two runs with different magnetic fields were made at each incident energy. These covered approximately E_x=0–13 MeV and E_x=13–30 MeV, with the exact energy ranges depending on the incident energy and spectrograph dispersion. The two spectra were then combined to form a continuous spectrum, samples of which are displayed in Fig. 1. The two spectra always had a region of overlap which provided a good check on our energy calibration and data-analysis procedures.

The proportional counter system consisted of two separate detectors, a thin (6-mm-deep) counter, used to determine position, followed by a thick (50-mm-deep) counter, used for particle identification via energy loss (ΔE). Position information was obtained by measuring the difference in rise times for pulses arriving at either end of the single high-resistance carbon-coated quartz anode. Both counters are enclosed in a large sealed box filled with argon (90%) and methane (10%) at a pressure of 1 atm. Particles enter this box through a thin (13-μm) aluminized Mylar window. The precise counter volumes (cathodes) are further defined by even thinner (3.7-μm) aluminized Mylar foils to which a high voltage of approximately 1500 kV is applied. A 0.05-mm-thick acetate foil was also placed in front of the counters to stop all elastically scattered ^{12}C ions since the count rate due to these ions is quite high at forward angles. Under ideal experimental conditions the counter is capable of 1 mm [full width at half-maximum (FWHM)] resolution with linearity better than 1%. This corresponds to $\Delta E/E \approx 10^{-3}$. In the present experiment, the resolution was limited to about 40 keV (FWHM), primarily by the energy spread of the incident ^{12}C beam and the target thickness.

The signals from the position and ΔE counters

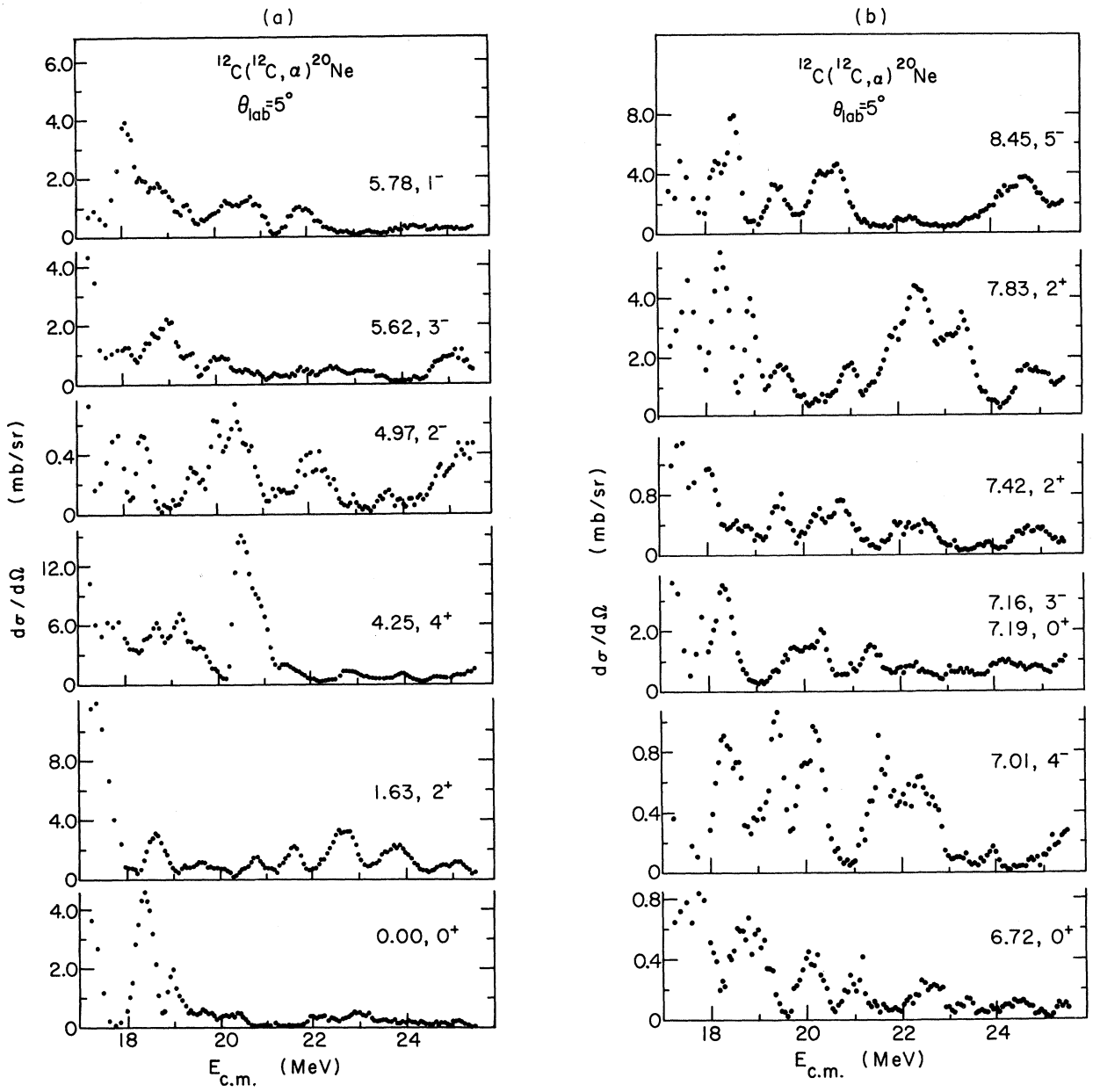

FIG. 2. Excitation functions at $\theta_{lab}=5°$ in the energy interval $E_{c.m.}(^{12}C)=18-25.5$ MeV for 22 levels in ^{20}Ne.

were analyzed in coincidence and stored in a 1024 ×32 array using an on-line computer. The spectra were plotted and transferred onto magnetic tape for subsequent analysis. The coincidence requirement between the two counters virtually eliminated all background due to γ rays, neutrons, or stray particles. The ΔE spectra were observed to contain <1% of particles other than α particles. In the off-line analysis of the position vs ΔE data matrix, the α ΔE peak could be light penned to produce a position spectrum containing virtually no contaminant particles.

III. EXPERIMENTAL RESULTS

The spectra were analyzed by eye through the use of a light pen. This procedure was facilitated by the fact that all known states in ^{20}Ne below ~9 MeV were observed with no measurable background. The resolution was not sufficient, however, to resolve the 7.166- (3^-) and 7.196- (0^+) MeV levels. For levels at higher excitation, the high density of unresolved and overlapping levels in ^{20}Ne produced a rising continuum of α particles. Since many levels have large natural widths

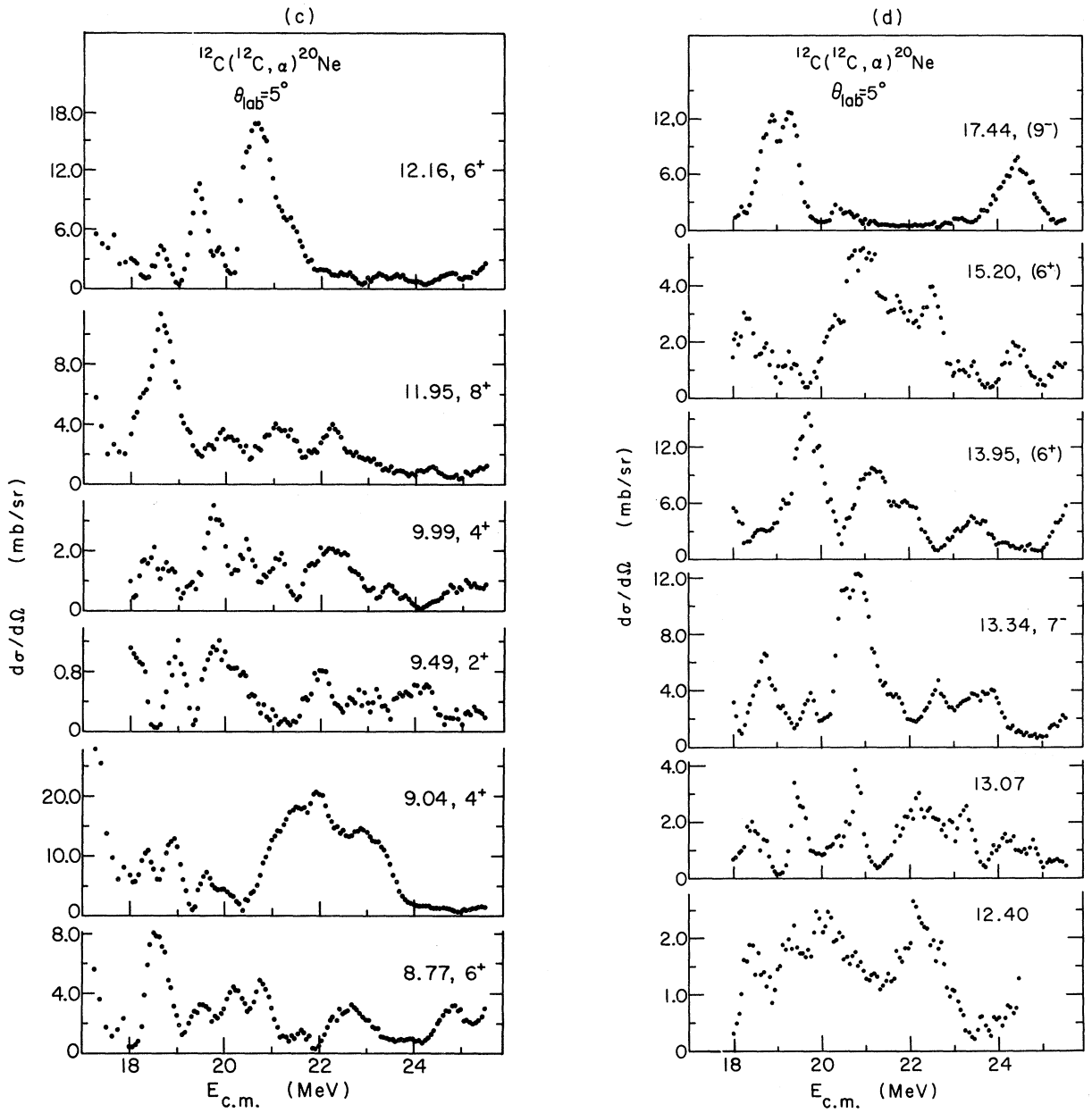

FIG. 2 *(Continued)*

(100–300 keV), it was extremely difficult to extract yields reliably for states such as the 10.60-(6⁻), 12.56- (6⁺), and 16.76-MeV levels. Strongly populated narrow peaks above ~9 MeV were analyzed by light penning the background under the peak and subtracting it out. Consequently, the errors in the measured yields were purely statistical for states below 9 MeV but for those at higher energies the error in background subtraction became quite large for weak yields, i.e., for cross sections $\lesssim 1$ mb/sr.

Excitation functions were obtained for about 30 levels in ^{20}Ne, although only 22 levels could be reliably analyzed over the entire energy range. In some energy regions, only upper limits were obtained for the remaining levels. The excitation functions are shown in Fig. 2. All of the observed levels and their average cross sections are listed in Table I.

Excitation energies were determined by calibrating the spectra using the known energies[9] for the low-lying states. The magnetic field of the spectrograph was varied to place these states at known distances along the focal plane. The re-

TABLE I. $^{12}C(^{12}C, \alpha)^{20}Ne$ average cross sections and results of statistical analysis of yield curves. The entry NS means a level was not seen, while W meant that while the level was observed it was too weak to be analyzed.

E_x [a] (MeV)	J^π [d]	$\left\langle \frac{d\sigma}{d\omega} \right\rangle$ [b] (mb/sr) Exp [e]	Hauser-Feshbach	Deduced [c] Y_d	Fluctuation results $R(0)$	Γ (keV)	Y_d
0	0^+	0.56	0.16	0.71	0.27	135	0.85
1.634	2^+	1.53	0.90	0.41	0.23	155	0.56–0.88
4.247	4^+	2.96	2.77	0.06	0.30	220	0 –0.83
4.968	2^-	0.24	0.14	0.42	0.27	160	0.68–0.85
5.622	3^-	0.69	0.84	···	0.13	180	0.78–0.93
5.785	1^-	0.74	0.11	0.85	0.21	195	0.89
6.722	0^+	0.21	0.031	0.86	0.28	130	0.85
7.006	4^-	0.37	0.57	···	0.26	150	0 –0.86
7.166 (weak)	3^-	1.00	0.53	(0.45)	0.14	180	(0.93)
7.196	0^+		0.028				
7.424	2^+	0.36	0.185	0.49	0.20	190	0.63–0.89
7.834	2^+	1.92	0.162	0.92	0.14	170	0.76–0.93
8.447	5^-	2.04	2.2	···	0.26	215	0 –0.86
(≈8.6)	0^+	NS	0.02				
(8.72)	1^-	NS	0.03				
8.775	6^+	2.43	4.0	···	0.24	220	0 –0.87
(≈8.8)	2^+	NS	0.12				
(8.82)	(5^-)	NS	1.8				
(8.850)	1^-	NS	0.027				
9.040	4^+	8.21	0.78	0.90	0.15	210	0.50–0.92
(9.117)	3^-	NS	0.30				
9.489	2^+	0.49	0.10	0.80	0.21	150	0.61–0.89
(9.950)	(1^+)	NS					
9.99	4^+	1.16	0.56	0.52	0.15	150	0.50–0.92
10.257	5^-	<1.0	1.33				
10.26	2^+		0.085				
10.55	4^+	<1.0	0.44				
10.61	6^-	NS	1.2				
10.84	$2^+, 3^-(2^+)$	<0.5					
10.92		<0.5					
11.01	4^+	W					
11.32	2^+	W					
11.53	≤ 4	W					
11.948	8^+	2.75	7.9	···	0.11	180	0 –0.94
(11.953) weak	(1^-)						
12.16	6^+	3.59	1.6	0.55	0.24	170	0 –0.87
12.40	$(3^-; 0^+)$	1.39			0.08	165	?
12.61	(6^+)	≈2					
12.75	4^+	W					
13.07	$(2^-; 4^+)$	1.34			0.28	145	?
13.34 13.333	7^-	3.65	2.5	0.32	0.16	205	0 –0.92
(13.342	4^+)						
13.70		W					
13.95	(6^+)	4.65	0.8	0.83	0.17	225	(0 –0.91)
14.35	(6^+)	2.85	0.68				
14.79		≈1.6					
15.20	(6^+)	1.97	0.4	0.80	0.16	170	(0 –0.92)
15.40		≈1.4					
15.62	(8^-)	NS	0.9				
15.93	$(5^-, 8^+)$	3.87					
16.75	(8^+)	≈1.6	1.25				
17.44	(9^-)	3.57	2.3	0.36	0.20	225	(0 –0.89)
18.15	$(6^+, 7^-)$	1.29					
18.50		2.54			0.15	130	(≤0.92)

TABLE I. *(Continued)*

[a] Excitation energies below 12 MeV are from the literature (Ref. 9); above 12 MeV they are from the present work.
[b] Averaged over the energy interval 36–51 MeV (lab).
[c] For comparison to the Ericson results, we calculate

$$Y_d = \left(\left\langle \frac{d\sigma}{d\omega} \right\rangle_{\text{exp}} - \left\langle \frac{d\sigma}{d\omega} \right\rangle_{\text{HF}} \right) \Big/ \left\langle \frac{d\sigma}{d\omega} \right\rangle_{\text{exp}} .$$

[d] Reference 9.
[e] NS denotes not seen; W denotes weak.

sultant curve of channel number versus focal plane distance was then fitted by a fifth order polynomial. This polynomial could then be used in the standard spectrograph analysis program QPLOT to obtain Q values. The excitation energies in Table I which are not denoted as being taken from other work[9] are estimated to be accurate within 10–30 keV, the error increasing with increasing excitation energy.

Absolute cross sections were determined by comparing the measured α yields to the yield of elastically scattered ^{12}C ions at an incident energy of 36 MeV. We were able to simultaneously record the 5^+ and 6^+ charge states of ^{12}C to obtain the total elastic yield. The measured elastic angular distribution deviated only slightly from Rutherford scattering at forward angles and agreed well with optical-model calculations using the potentials of Malmin *et al.*[10]

The absolute cross sections were also corrected for carbon buildup on the target, which was determined by repeating certain points on the excitation function at well-separated time intervals. These corrections were less than 10%, except for one series of runs when the spectrograph vacuum was particularly poor and a 30% buildup was observed. Finally, the normalization procedure was checked by comparing repeat points between series of runs and between the states that overlapped on the low- and high-energy excitation runs. The relative cross sections are accurate within 10% for $d\sigma/d\omega > 1$ mb/sr. Absolute cross sections are estimated to be accurate to within 30%. The cross sections to each level, averaged over the entire interval (36–51 MeV), are listed in Table I and shown in Fig. 3.

Several important points are apparent from an inspection of the excitation functions shown in Fig. 2. All of the excitation functions show strong variations in the yield as a function of energy. The

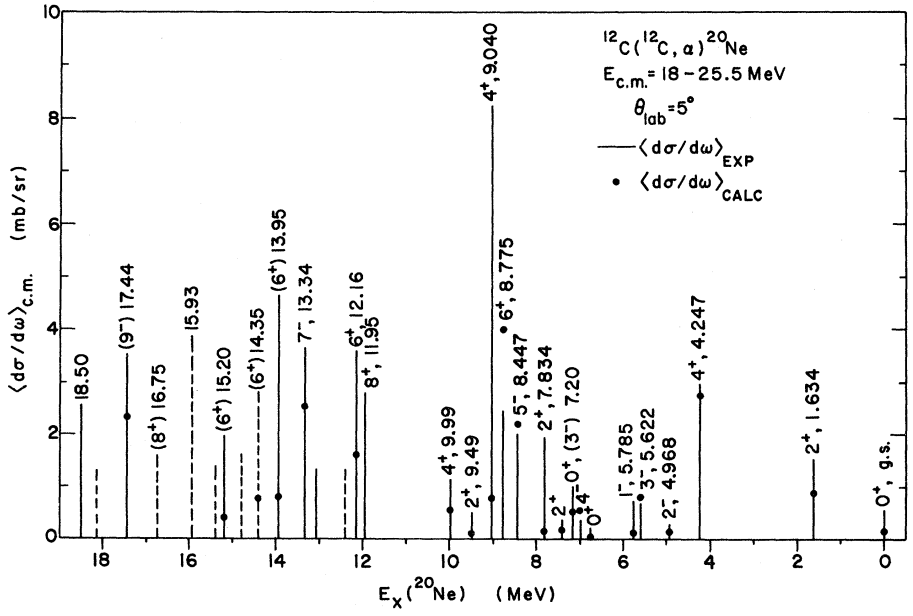

FIG. 3. The energy-averaged experimental (vertical lines) cross sections ($\theta_{lab} = 5°$, $E_{c.m.}(^{12}C) = 18–25.5$ MeV) are compared to statistical compound-nuclear Hauser-Feshbach cross sections (dots). The theoretical values were computed assuming $W(\theta) \propto 1/\sin\theta$. Dashed lines are for states whose peaks were not apparent at all energies.

structure is most pronounced at the lower bombarding energies and is considerably damped out as the incident energy increases, especially for states of low spin and/or low excitation energy. In the bombarding energy region, 18–20 MeV, several of the states show maxima that appear to be correlated. A statistical analysis of the correlations of the structure in the yield curves is presented in Sec. VI. The widths of the peaks in the excitation functions vary greatly from level to level and from energy to energy, but usually fall in the range 0.3–0.8 MeV (c.m., FWHM). The magnitudes of the peaks also vary greatly, with peak-to-valley ratios ranging from 2 : 1 up to 120 : 1. Such large fluctuations with relatively narrow widths clearly indicate the presence of a significant statistical compound-nuclear reaction component. However, a nonstatistical component is also suggested by the apparent correlations of individual resonances between different channels.

A nonstatistical reaction component is apparent also from the energy-averaged magnitudes of the cross sections (Table I and Fig. 3). Over all, the average cross sections increase with the spin of the final state and decrease with excitation energy. There are, however, some notable exceptions. There are two close-lying 0^+ states (6.72 and 7.20 MeV), two 2^+ states (7.42 and 7.83 MeV), two 4^+ states (9.04 and 9.99 MeV), and two 6^+ states (12.16 and 12.56 MeV). In all four cases, two states of the same spin and parity at nearly the same excitation energy have cross sections which differ by about a factor of 5. It is thus clear that the mechanism which populates these states is nonstatistical since it depends on more than just the spin, parity, and excitation energy of the levels. These data suggest that the stronger set of states is being populated by a direct 8-nucleon transfer reaction which is consistent with their being members of a proposed[5] 8p-4h structure for this band. Even for the strong states, however, the cross section possesses strong fluctuations which can be attributed to interference between the direct and compound processes.

There are several other striking examples of nonstatistical effects in the average cross sections. It is also interesting to note the large cross sections to the members of the 2^- band beginning at 4.968 MeV. These points will be discussed in detail in Sec. VIII.

IV. ANGULAR DISTRIBUTIONS

Angular distributions were measured at five energies, $E_{lab} = 37$, 41, 45, 48, and 51 MeV. Spectra were obtained in 1° or 2° steps in the angular interval 5°–30° and then in 5° steps up to 80°. Since the incident projectile and the target nucleus are identical, angular distributions must be symmetric about 90° in the center-of-mass system, regardless of the reaction mechanism. Hence it was necessary to make measurements only at lab angles $\lesssim 80°$ to obtain complete angular distributions.

Since the energy of the outgoing α particle falls rapidly with increasing angle, the excitation energy range spanned by the counter length (50 cm) also decreases. For this reason, we have only partial angular distributions for states above 9 MeV in excitation, but complete distributions at all energies for all levels in the excitation energy range $E_x = 0$–9 MeV. Angular distributions at 45 MeV for all levels are shown in Fig. 4. Angular distributions at all five energies are shown for three of the states in Fig. 5.

The shapes of the angular distributions change greatly from energy to energy as well as from level to level. In a purely direct reaction, the angular distribution for feeding a level with a given spin and parity would be expected to exhibit a characteristic pattern which varies slowly with bombarding and/or excitation energy. The observed fluctuations presumably arise from that part of the reaction which proceeds through strongly overlapping levels of the compound nucleus. However, this does not mean that the reaction mechanism is mainly compound nuclear since a relatively small compound-nuclear component can, through interference, strongly influence the angular distributions.

Each distribution was fitted by a Legendre polynomial series:

$$\frac{d\sigma}{d\omega} = \sum_{l\,\text{even}} A_l P_l(\cos\theta) = A_0\Big[1 + \sum_{\substack{l\,\text{even}\\ l\geq 2}} a_l P_l(\cos\theta)\Big]$$

including terms up to P_{18}. The resultant fits are shown by the solid lines in Fig. 4.

All of the angular distributions were analyzed for fluctuations to determine the average coherence angle, using the relation

$$R_\theta(\epsilon) = \frac{\langle \sigma(\theta)\sigma(\theta+\epsilon)\rangle}{\langle \sigma(\theta)\rangle\langle \sigma(\theta+\epsilon)\rangle} - 1,$$

where $\sigma(\theta)$ is the measured differential cross section at angle θ. Since θ must be stepped in equal increments in the center-of-mass system, $\sigma(\theta)$ was determined from the Legendre polynomial fits. The distributions were averaged by the method of moving averages. Ericson[11] has shown that for a reaction proceeding through overlapping uncorrelated compound nucleus levels $R(\epsilon)$ will be a Lorentzian whose half-width is equal to the average coherence angle designated β. Consistent values

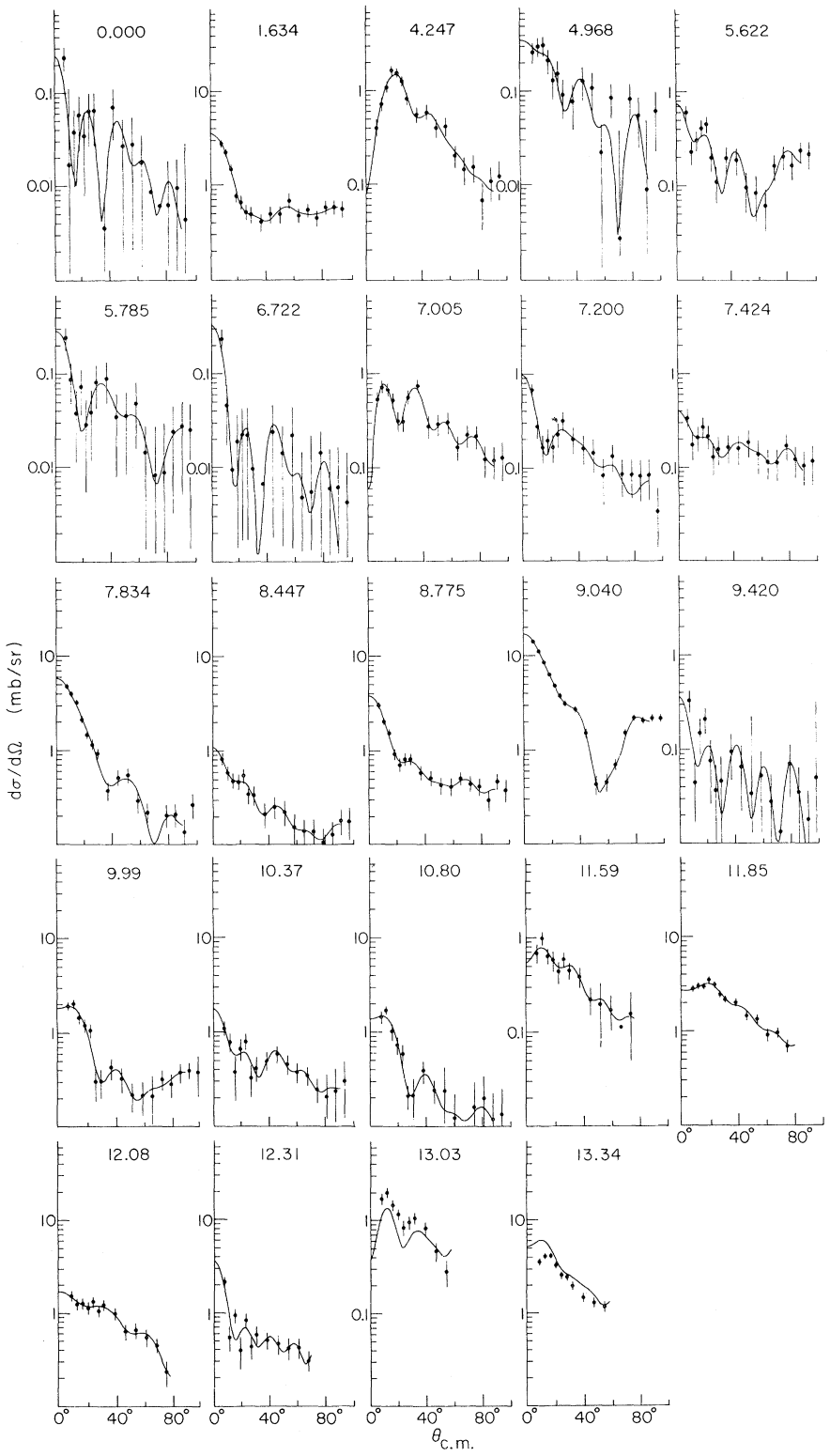

FIG. 4. Center-of-mass angular distributions observed at a (lab) bombarding energy of 45 MeV. The solid lines are Legendre polynomial fits with even terms up to P_{18} included.

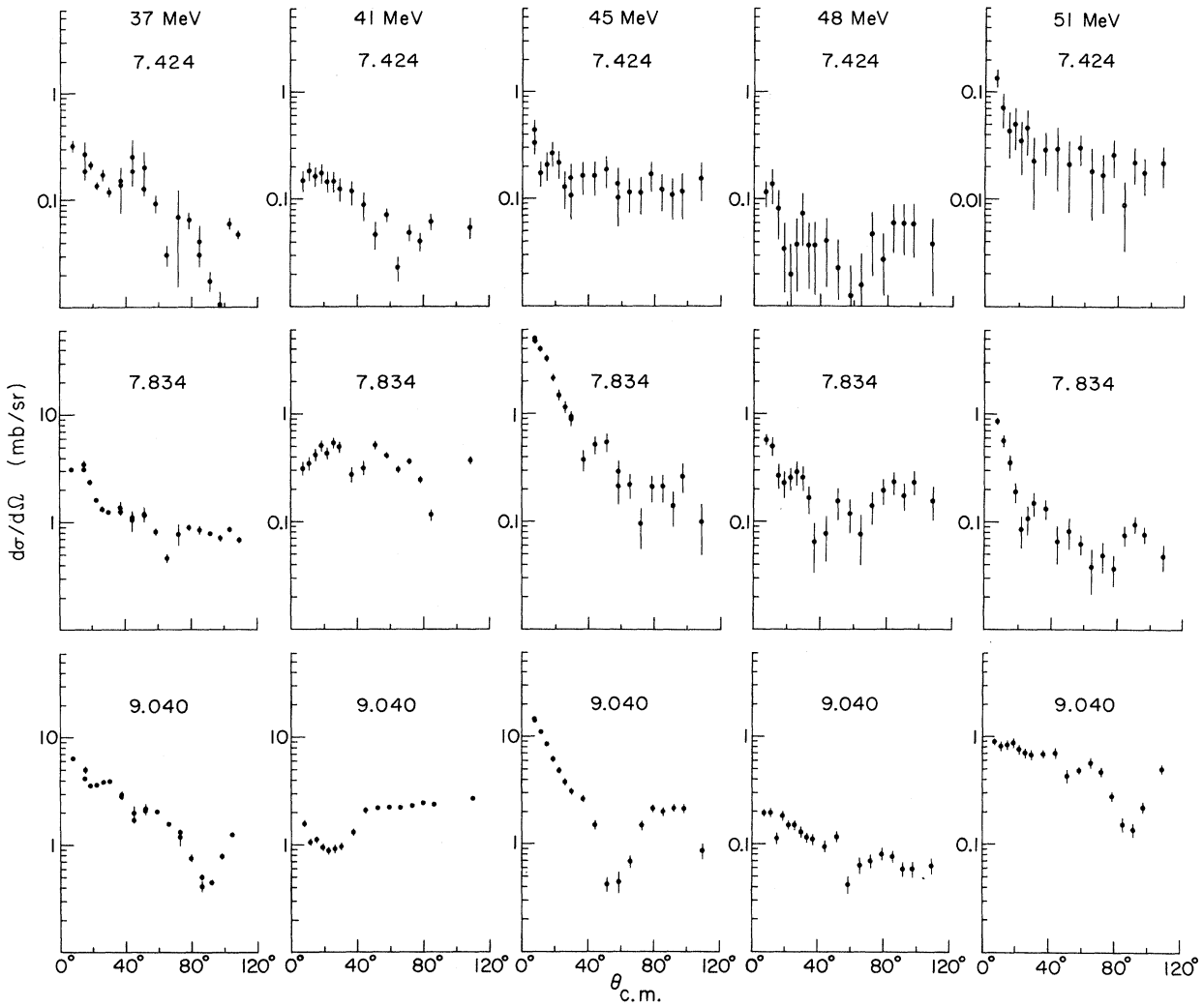

FIG. 5. Center-of-mass angular distributions taken at five bombarding energies of the α particles feeding the 7.42-MeV (2^+), 7.83-MeV (2^+), and 9.04-MeV (4^+) states.

of β were found over a wide range of averaging intervals. All levels at all energies gave values of β between 4 and 9°. These values of β are compatible with simple compound nuclear-models of Ericson[11] or Brink[12] which predict that $\beta \approx (kR)^{-1} \approx (l_{\max})^{-1}$ (e.g., $l=6$ would predict $\beta \approx 10°$ and $l=10$ would predict $\beta \approx 6°$).

There does not appear to be any increase in the value of β for those states which exhibit large cross sections such as those in the proposed (8p-4h) band starting at 7.2 MeV. If these states have a predominant direct reaction mechanism, it might be expected that they would have larger coherence angles. However, this lack of increase in β agrees with the lack of increase, noted below, in either the coherence width Γ or the mean square deviation $R(0)$ for these states. The Ericson analysis thus appears to be sensitive only to the narrowest fluctuations, which, of course, are produced by the compound-nucleus formation.

Several other considerations might also hamper the extraction of a meaningful larger coherence angle. First the angular distributions cannot be properly averaged at small angles as angles less than 0° are unphysical. Since we expect the major effects of a direct component to appear at small angles, our averaging procedure might well reduce these effects. Secondly, the angular distributions are required to be symmetric about 90°, regardless of the reaction mechanism, thus making the distinction between direct and compound effects harder to extract. Finally, we do not really know what type of oscillations to expect in a purely direct mechanism. Direct 1-α transfers in this

mass region show oscillations with periods less than 10°.[13] Preliminary calculations using the LOLA[14] code for the present reaction predict somewhat more gradual oscillations with periods of 10–20°.

In order to study the average behavior of the angular distributions as a function of bombarding energy, the five distributions for each level were added together. Of course this procedure may not be sufficient to guarantee representative energy-averaged angular distributions since only five measurements at rather widely separated energies were made. Nevertheless, it is hoped that these composite distributions average over the fluctuations sufficiently that the resulting angular distributions might be compared to predictions for direct and compound-nuclear reactions. Since the center-of-mass angles change significantly from energy to energy, the Legendre coefficients (A_l above) rather than the actual data have been added in order to obtain a composite angular distribution for each level. This procedure may introduce some smoothing of the data, although from the quality of the fits, as seen in Fig. 4, it appears that little detail was lost. The composite angular distributions are shown in Fig. 6 and the summed coefficients are listed in Table II.

A striking feature of the composite distributions is the strong oscillations for α particles feeding the ground and 6.72-MeV states, both of which are 0^+. Weaker and more widely spaced oscillations appear in the α particles feeding the other 0^+ state which is at 7.20 MeV. For the ground state large components up to and including P_{18} (the highest order Legendre polynomial included in the summation) are indicated. Thus, $l \geq 10$ must be present in significant proportions (odd l cannot contribute to a reaction when all of the particles are 0^+ and either the initial or the final state consists of identical particles). The distribution to the 6.72-MeV

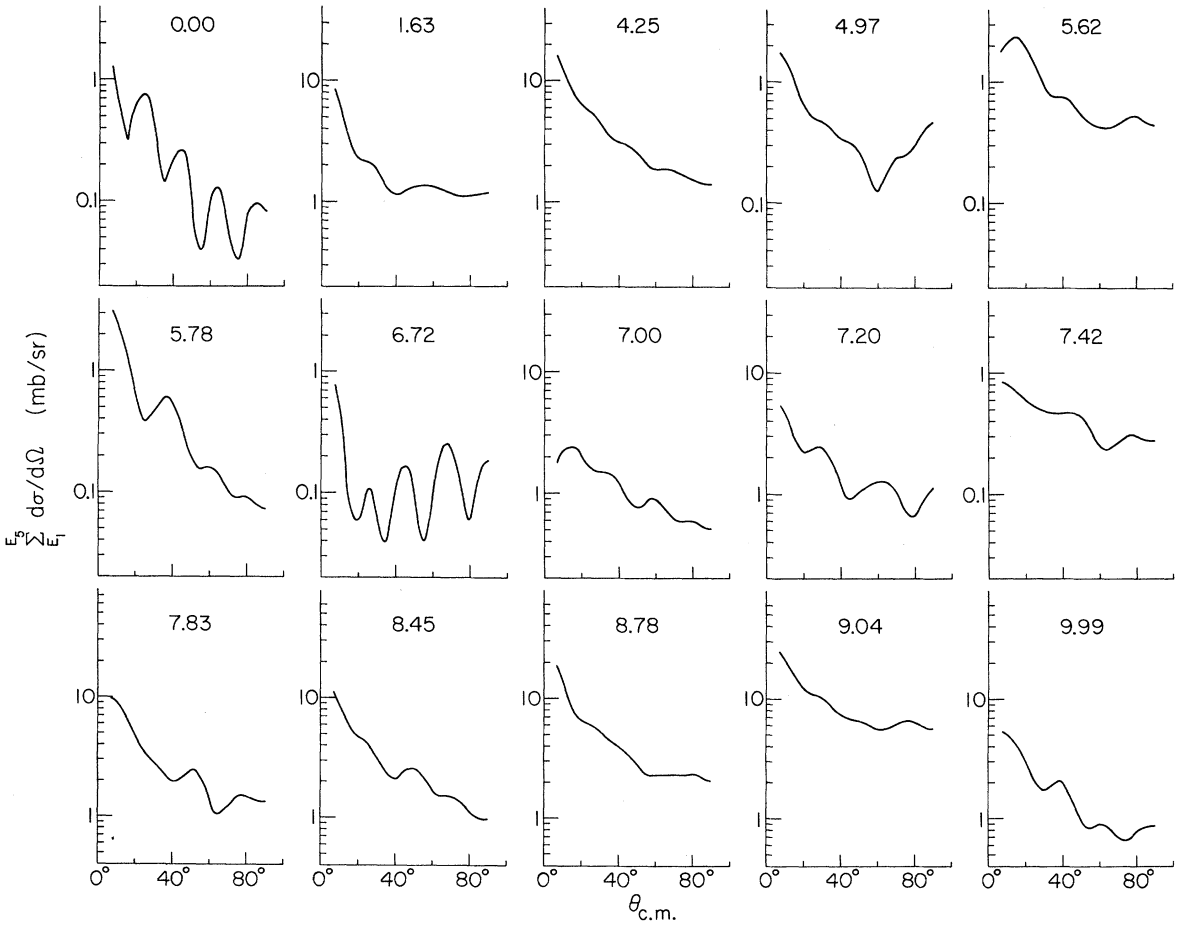

FIG. 6. Composite angular distributions for all of the levels below 10 MeV excitation energy that were studied in the present work. The composites were formed by adding the un-normalized Legendre coefficients obtained for each level at each bombarding energy.

TABLE II. Average normalized Legendre coefficients a_l for all levels for which complete angular distributions were taken at all five energies. The quantities a_l were defined by $a_l \equiv [\sum_E A_l(E)]/[\sum_E A_0(E)]$.

E_x (MeV)	$\bar{\sigma}$ (mb)	a_2	a_4	a_6	a_8	a_{10}	a_{12}	a_{14}	a_{16}	a_{18}
0.00	0.48	2.07	1.53	0.60	0.48	0.37	0.97	1.43	2.84	2.27
1.63	3.78	0.85	1.00	1.10	0.84	0.60	0.77	0.66	0.46	0.15
4.25	7.23	1.46	1.06	0.84	0.62	0.57	0.39	0.42	0.42	0.15
4.97	0.89	0.98	1.52	0.40	1.07	0.54	0.35	0.05	0.27	−0.38
5.62	1.74	1.17	1.01	0.30	0.01	−0.32	−0.73	−0.40	−0.20	0.10
5.79	0.80	2.34	1.80	1.69	2.13	2.20	1.21	−0.01	−0.23	0.11
6.72	0.33	0.03	0.69	1.35	0.74	1.61	1.08	−0.22	2.51	0.00
7.00	2.40	1.04	0.38	0.12	−0.21	−0.15	−0.02	−0.36	−0.47	0.04
7.20	3.40	1.04	0.76	0.63	0.19	0.30	1.09	0.23	0.23	−0.25
7.42	0.94	0.72	0.26	−0.00	0.39	0.15	−0.25	0.14	0.00	−0.08
7.83	5.50	1.24	1.00	0.84	0.83	0.11	−0.12	0.35	−0.18	−0.27
8.45	5.63	1.34	0.76	0.93	0.63	0.29	0.18	0.57	0.40	−0.05
8.78	8.73	1.25	1.07	0.70	0.68	0.81	0.56	0.47	0.35	0.25
9.04	18.83	0.74	0.73	0.39	0.30	0.35	0.14	0.27	0.03	−0.01
9.99	3.30	1.33	0.92	0.40	0.63	0.45	0.11	−0.55	−0.26	0.17

state contains a large P_{16} term while the P_{18} term does not differ significantly from zero. However, $|P_8|^2$ does not give a particularly good fit to the data thus indicating the presence of more than one intermediate state.

Two low-lying unnatural-parity states were formed: the 4.97-MeV 2^- state and the 7.01-MeV 4^- state. Cross sections for feeding such states by the $^{12}C(^{12}C, \alpha)$ reaction must vanish at 0°. For the 7.01-MeV state the distribution does turn over at about 15° and appears to be heading for a null value at 0°. However, no such behavior is apparent for the 4.97-MeV state. It is possible that the 0° dip for this state is too sharp to have a significant effect in the present work in which the most forward angle was about 7.5° c.m. Indeed, in the 45-MeV data (Fig. 4) for this state there is an indication of a turnover at very small angles which is not picked up by the Legendre fit.

Since all of the angular distributions show forward or near forward peaking most of the Legendre coefficients are positive. On the average, the magnitudes of the coefficients decrease with increasing order, as would be expected if a large number of angular momenta are present. Outside of the oscillations in the distributions to the 0^+ states noted above, there is no obvious feature which can be tied to the final state spin. Neither are there obvious similarities in the distributions to states in the same rotational band.

When a large number of angular momentum waves are participating in a statistical compound-nuclear reaction the average angular distributions will be closely approximated[15] by $W(\theta) \sim 1/\sin\theta$. We have thus also obtained the composite angular distributions leading to all levels $E_x \leq 9.04$ MeV at

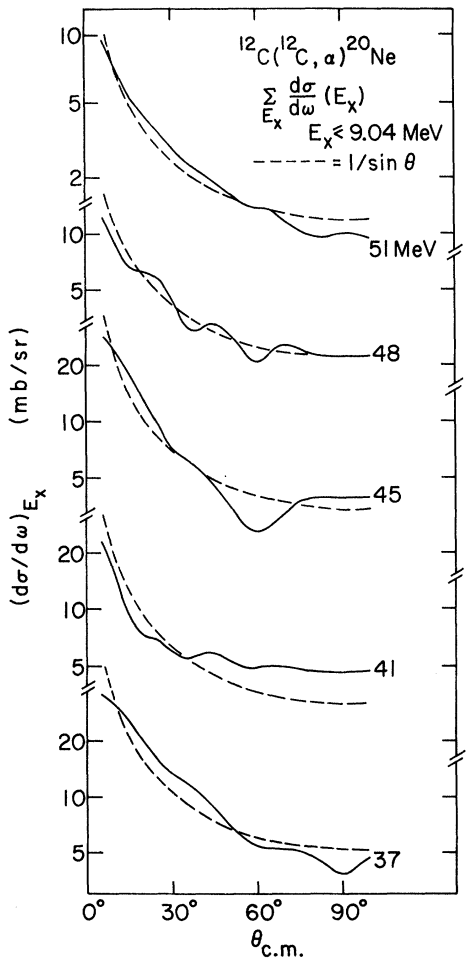

FIG. 7. Total angular distributions for feeding all of the levels up to and including the one at 9.04 MeV.

each of the five energies. These distributions are shown in Fig. 7 where they are compared to $1/\sin\theta$. While deviations from a $1/\sin\theta$ shape are clearly present, these deviations do not appear to be systematic and may be ascribed to the finite number of levels whose distributions are being averaged. However, this similarity to a $1/\sin\theta$ shape may not be a good test of the reaction mechanism since direct angular distributions are also forward peaked and in the present case must also be symmetric about 90°.

V. FLUCTUATION ANALYSIS

A striking feature of the excitation functions is the large variations in yield observed over small changes in energy. Such behavior is taken to indicate the presence of statistical compound-nuclear processes. In order to quantitatively determine the relative strength of "direct" and compound-nuclear mechanisms, we have analyzed the measured excitation functions in terms of Ericson fluctuations.[11] The methods detailed by Greenwood *et al.*[3] have been followed closely.

Autocorrelations were calculated from the relation

$$R_E(\epsilon)=\frac{\langle\sigma(E)\sigma(E+\epsilon)\rangle}{\langle\sigma(E)\rangle\langle\sigma(E+\epsilon)\rangle}-1, \tag{1}$$

where $\sigma(E)$ is the measured differential cross section at energy E, ϵ is the energy interval, and Γ is the average coherence width $\langle\Gamma_I\rangle$. Average cross sections $\langle\sigma\rangle$ were calculated by the method of moving averages. Consistent values of $R(\Gamma, 0)$ and Γ were found with an averaging interval of about 1.56 MeV (c.m.). The coherence width Γ was determined from the half-width of the autocorrelation function using the relation

$$R(\epsilon)=\frac{\Gamma^2}{\Gamma^2+\epsilon^2}\,\frac{[1-Y_d^{\,2}]}{N_{\rm eff}}$$
$$=\tfrac{1}{2}R(\Gamma,0)\ \text{ at }\epsilon=\Gamma, \tag{2}$$

where $N_{\rm eff}$ is the effective number of open channels and Y_d is the ratio of the average direct cross section to the average total cross section. In the present discussion the term direct does not necessarily imply multinucleon transfer without the formation of a compound nucleus but rather includes all processes which take place in a time short compared to $\hbar/\Gamma$. The resulting values of $R(\Gamma, 0)$ and Γ are listed in Table I. [Note that the shape of $R(\Gamma, \epsilon)$, and therefore the value of Γ, is independent of $N_{\rm eff}$ and Y_d.]

The average coherence widths Γ are about 150–200 keV (c.m.) and appear to increase with the spin of the final state, as would be expected in a compound-nuclear process.[3] These values are consistent with previous studies[1,2] for the present reaction as well as with the value of $\Gamma\approx 100$ keV found in the $p+{}^{23}$Na reaction for lower energies in ^{24}Mg (Refs. 10, 16, and 17) when the fact that Γ is expected to increase slowly with excitation energy in the compound nucleus is taken into account.

Utilizing Eq. (2), the autocorrelation coefficients or mean square deviations $R(\Gamma, 0)$ can be taken as a measure of the direct-reaction component Y_d. However, the interpretation is complicated by needing to know the number of effective open channels $N_{\rm eff}$ and this quantity is difficult to determine precisely. Generally $1\leq N_{\rm eff}\leq(I+1)$, where I is the spin of the final state. At 0° $N_{\rm eff}=1$ and it is a maximum at 90°. At $\theta_{\rm c.m.}\approx 7.5°$ we expect $N_{\rm eff}$ to be less than half of the average of the minimum (≡1) and the maximum allowed values.[1-3]

For the 0^+ states $N_{\rm eff}=1$ at all angles. Thus, from the extracted values of $R(\Gamma, 0)$ we can conclude that $Y_d=0.85$, both for the ground state and for the 6.722-MeV level. For the 0^+ 7.196-MeV level Y_d is also large. However, the weaker 7.166 (3^-) state is not fully resolved and its presence makes it difficult to estimate Y_d for the 7.196-MeV state.

The ground-state analysis is shown graphically in Fig. 8 where the frequency distribution of the deviation of the cross section from the average is plotted. Since $N_{\rm eff}=1$ ($J^\pi=0^+$), we expect[11]

$$P(Y)=\frac{1}{(1-Y_d)}\exp\left[-\left(\frac{Y+Y_d}{1-Y_d}\right)\right]I_0\left[\frac{2\sqrt{Y}\,Y_d}{(1-Y_d)}\right], \tag{3}$$

where $Y=\sigma/\langle\sigma\rangle$ and I_0 is a modified Bessel func-

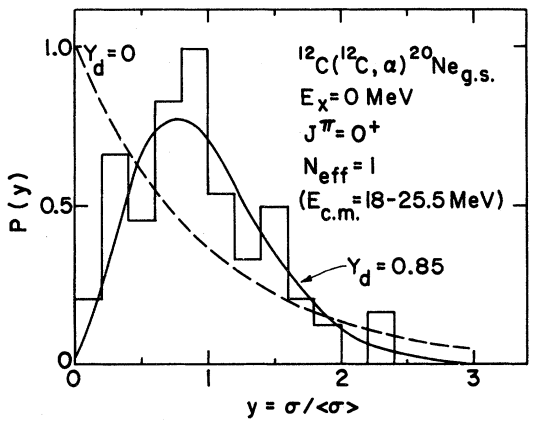

FIG. 8. Frequency histogram for the ratio of $\sigma/\langle\sigma\rangle$ for the ground state, where $\langle\sigma\rangle$ is the energy-averaged cross section (averaging interval = 1.56 MeV). Since $J^\pi=0^+$, $N_{\rm eff}=1$. The dashed curve assumes $Y_d=0$ (purely statistical compound nuclear). The solid curve was calculated using Eq. (3) of the text with $Y_d=0.85$.

tion. In a purely statistical compound-nuclear reaction $Y_d = 0$ and this expression reduces to $P(Y) = e^{-Y}$. As shown in Fig. 8, the measured distribution $P(Y)$ requires a large Y_d; it is well fitted by $Y_d = 0.85$.

For higher-spin states, Table I gives the full range of values of Y_d that are allowed by the range of N_{eff}, although the lower limits on Y_d are probably too low since N_{eff} is expected to be less than half of the maximum allowed value. Even so, it is apparent that most of the states require a large direct-reaction component. This result is in contrast to earlier studies[1,2] which found that the ground-state and first-excited-state fluctuations were well described by a purely statistical compound-nuclear reaction mechanism. However, those studies were at a much lower energy where the compound-nuclear cross sections are at a maximum. Since the compound-nuclear cross sections fall rapidly with energy, as will be shown in Sec. VII, the direct-reaction fraction should increase with energy.

Evidence that the fraction of direct component increases with energy is also found directly in the data. The sum of the deviations from the average for all of the measured excitation functions is shown in Fig. 9. There it can be seen that the magnitude of the absolute deviation

$$D'(E) = \sum_i \left(\frac{\sigma_i(E)}{\langle \sigma(E) \rangle_i} - 1 \right), \tag{4}$$

where i refers to different states in ^{20}Ne, on the average falls with increasing energy. Since Y_d is inversely related to the deviations, Y_d must be increasing with energy.

It is noteworthy that the $R(\Gamma, 0)$ values for the states of the $K^\pi = 0^+$ band that starts at 7.196 MeV are only slightly lower than those for the nearby $K^\pi = 0^+$ band starting at 6.722 MeV, even though the 7.196 band is excited much more strongly. Also, the large values of Y_d found for states of the $K^\pi = 2^-$ band are perhaps surprising since in many of the possible direct reactions unnatural-parity states cannot be populated. Perhaps both of these anomalies are manifestations of the inaccuracies of the Ericson method for determining the relative magnitude of the direct and compound-nuclear cross sections. Statistical errors, including those due to finite size of data, are in all cases less than 20%. It is estimated that the total errors in $R(\Gamma, 0)$ and Γ are less than 30%, even at high excitation energies where the presence of weak unresolved levels could tend to fill in the minima and cause systematic errors in the determination of the cross sections. For the small values of $R(\Gamma, 0)$ determined here, an error of 30% would still allow an accurate measurement of Y_d, since $Y_d = [1 - R(\Gamma, 0)N_{\text{eff}}]^{1/2}$. For example, if $N_{\text{eff}} = 1$ and $R(\Gamma, 0) = 0.3$ $\Delta R/R = 0.3$ implies

$$\frac{\Delta Y_d}{Y_d} = \tfrac{1}{2} \frac{R}{[1-R]} \frac{\Delta R}{R} = 0.064.$$

However, it is not to be expected that an Ericson analysis can determine the magnitude of the direct component to such a high degree of accuracy. A more realistic view would be that the present

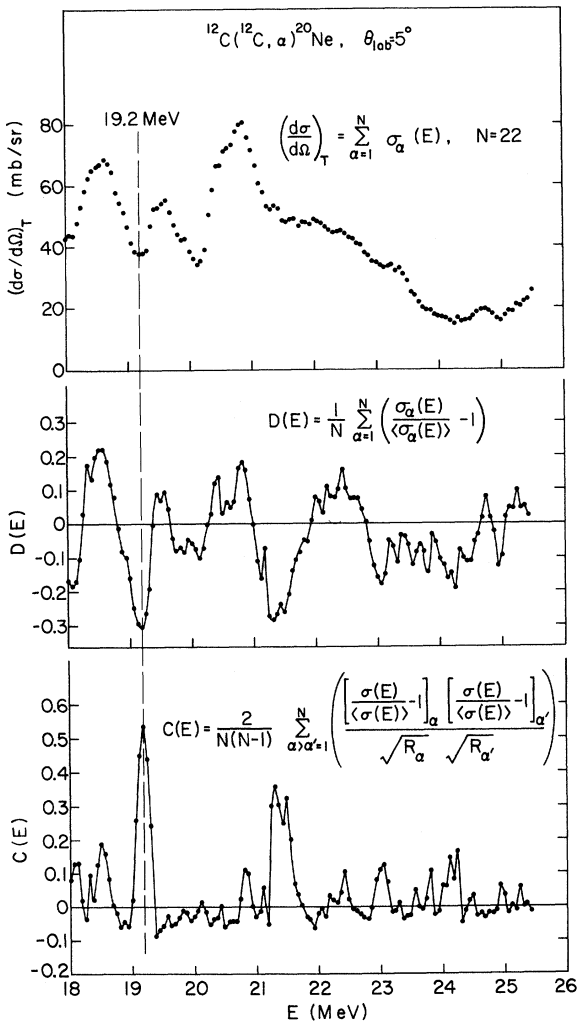

FIG. 9. (a) The 22 excitation functions are added together to show the total α cross section at $\theta_{lab} = 5°$. (b) The deviations of the cross sections from the energy-averaged ($\Delta = 1.56$ MeV) cross sections are added together for all 22 levels. (c) The cross correlations for each pair of levels (231 in all) are added together at each energy. Note the large peak in (c) at 19.2 MeV. This corresponds to a large dip in (a) and (b) indicating the presence of a large correlated *minimum*. This is close to the large correlated *maximum* found by Ref. 7 in the $^{12}C(^{12}C, p)^{23}Na$ reaction.

statistical analysis supports the conclusion that the $^{12}C(^{12}C, \alpha)^{12}Ne$ reaction is predominantly direct, but that the degree to which the direct component dominates can only be roughly estimated. Furthermore, the present analysis says nothing about the nature of the direct or nonstatistical component. In a recent study of various $^{12}C + ^{12}C$ reactions at similar energies to those used here, Shapria, Stokstad, and Bromley[18] found values of Γ similar to those reported here. These authors also report large nonstatistical components in the six selected α particle exit channels that they studied.

VI. CORRELATION ANALYSIS AND SEARCH FOR CONTINUUM STRUCTURE

It is also of interest to look for cross correlations between the excitation functions for different levels. Van Bibber *et al.*[7] have recently found evidence that structure in the excitation functions of several levels in the $^{12}C(^{12}C, p)^{23}Na$ reaction are strongly correlated at several energies, especially near $E_{c.m.} = 19.3$ MeV. Thus, there may be strong resonances in the $^{12}C + ^{12}C$ system similar to those reported by Malmin *et al.*[10] for the $^{12}C + ^{16}O$ system (near $E_{c.m.} = 19.7$ MeV).

All of the 22 measured excitation functions were analyzed for cross correlations using the relationship

$$R_\epsilon(\alpha, \alpha') = \frac{\langle \sigma_\alpha(E)\sigma_{\alpha'}(E+\epsilon)\rangle}{\langle \sigma_\alpha(E)\rangle\langle \sigma_{\alpha'}(E+\epsilon)\rangle} - 1 , \tag{5}$$

where α, α' refer to different states in ^{20}Ne, and ϵ is the energy interval. The cross correlations were then normalized by

$$C_{\epsilon=0}(\alpha, \alpha') \equiv \frac{R_{\epsilon=0}(\alpha, \alpha')}{[R_{\epsilon=0}(\alpha) R_{\epsilon=0}(\alpha')]^{1/2}} , \tag{6}$$

where $R_{\epsilon=0}(\alpha)$ is the autocorrelation coefficient $R(\Gamma, 0)$ defined by Eq. (1). All correlations were performed with a 25 point ($\Delta E_{c.m.} = 1.56$ MeV) moving average. The resultant frequency distribution of the values of $C_{\epsilon=0}$ are shown in Fig. 10. The dashed line is the Gaussian distribution predicted for statistical or uncorrelated fluctuations.[1,2] As can be seen, the fit is excellent leading to the conclusion that most of the observed structure in the excitation functions is statistically uncorrelated.

Since 22 levels were analyzed in the above manner (resulting in 231 cross correlations), it is possible that some subset of the levels possesses a consistent pattern of correlations that is masked. Therefore, we have also looked at cross correlations as a function of J^π and rotational band assignment in ^{20}Ne. Again we find no pattern of correlations when the entire energy range is included in the analysis.

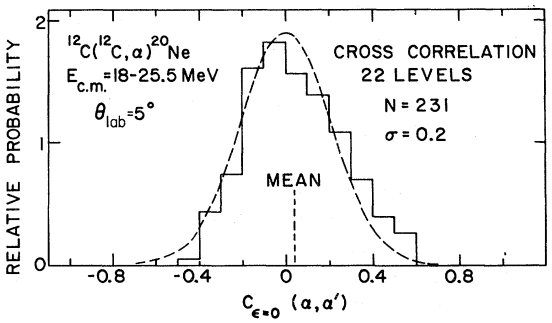

FIG. 10. The distribution of the energy-averaged cross correlations of the 22 excitation functions, defined by Eqs. (5) and (6) in the text. The mean value is close to zero and the dashed curve is the expected distribution assuming that the excitation functions have random, uncorrelated fluctuations.

A search has been carried out for isolated resonances such as those reported by Van Bibber *et al.*[7] and Malmin *et al.*[10] A small number of such resonances could be missed in the analysis described above when the data over the full energy range are included. In order to search for such isolated resonances, the data have been analyzed in three ways. First, the sum of the cross sections to all 22 levels was determined as a function of incident energy:

$$\sigma(E) = \sum_{i=1}^{22} \sigma_i(E) . \tag{7}$$

Then the deviations from the average were added, using the same averages as employed in the Ericson analysis:

$$D(E) = \frac{1}{N} \sum_{\alpha=1}^{N} \left[\frac{\sigma_\alpha(E)}{\langle \sigma_\alpha(E)\rangle} - 1 \right] . \tag{8}$$

(The absolute value of the deviations was not used, since it can be easily shown that this procedure leads to a discontinuous frequency distribution, e.g., if $P(y) = e^{-y}$, then $D = |y - 1|$ will rise for $0 < y < 1$, have a sharp discontinuity at $y = 1$, and fall as e^{-y} for $y > 1$.) Finally, the summed normalized cross correlations as a function of energy were obtained:

$$C(E) \equiv \frac{2}{N(N-1)} \sum_{\alpha,\alpha>\alpha=1}^{22} \left\{ \left[\frac{\sigma_\alpha(E)}{\langle \sigma_\alpha(E)\rangle} - 1 \right] \Big/ \sqrt{R_\alpha} \right\} \left\{ \left[\frac{\sigma_{\alpha'}(E)}{\langle \sigma_{\alpha'}(E)\rangle} - 1 \right] \Big/ \sqrt{R_{\alpha'}} \right\} , \tag{9}$$

where R_α is the autocorrelation coefficient defined previously. All three functions are shown together in Fig. 9.

The most striking feature in Fig. 9 is the narrow cross-correlation peak at $E_{c.m.}=19.2$ MeV.[19] This energy is close to that reported by Van Bibber *et al.*[7] for the resonance in the $^{12}C(^{12}C,p)^{23}Na$ channel. A difference in energy of 100 keV is well within the combined uncertainties in the absolute energy calibration of the Brookhaven and Argonne tandem accelerators for heavy ions. The width of the correlation peak is about 250 keV, implying a resonance width of about 500 keV (c.m.), which also agrees with the width observed for the proton resonance.[7] [For two completely correlated Breit-Wigner resonances of width Γ, the width obtained in $C(E)$ from Eq. (9) will be 0.62Γ. Thus a width of 250 keV in $C(E)$ implies a resonance width of 400 keV or more.]

Both the cross-section sum and the deviation sum display a minimum at this energy. The cross-correlation peak is thus due to the product of two negative numbers, i.e., dips in the cross sections. An examination of the excitation functions to individual levels shows that about $\frac{2}{3}$ of them possess a minimum near 19.2 MeV. Most of the remaining do not show any peaks at this energy, but for these cases 19.2 MeV is usually on the side of a nearby peak. It thus appears that there may be a loss of flux in the α channel due to the large resonance in the proton channel. These results support the interpretation in Ref. 7 that the resonance has a microscopic configuration which strongly favors proton decay to ^{23}Na. However, since it is energetically possible for the ^{24}Mg compound state to decay by α emission to many states in ^{20}Ne, it is hard to understand why none of the α peaks resonate at the appropriate energy. More work is needed to understand the precise nature of the observed resonance at 19.2 MeV.

Three distinct peaks occur in various excitation functions in the bombarding-energy range 18–19.5 MeV. Very few of the excitation functions possess all three, but most states show at least one. An analysis of these resonances appears elsewhere.[20]

Finally, the position of the 8^+ members of various bands is unknown, except for the ground state band. The present experiment has little to say about these high-spin states except that a strongly excited state at ~16.6 MeV is a strong candidate for the 8^+ member of the 8p-4h band. If such is the case, the possibility exists that this state would have a measurable α decay to the 0^+ state at 6.06 MeV in ^{16}O.

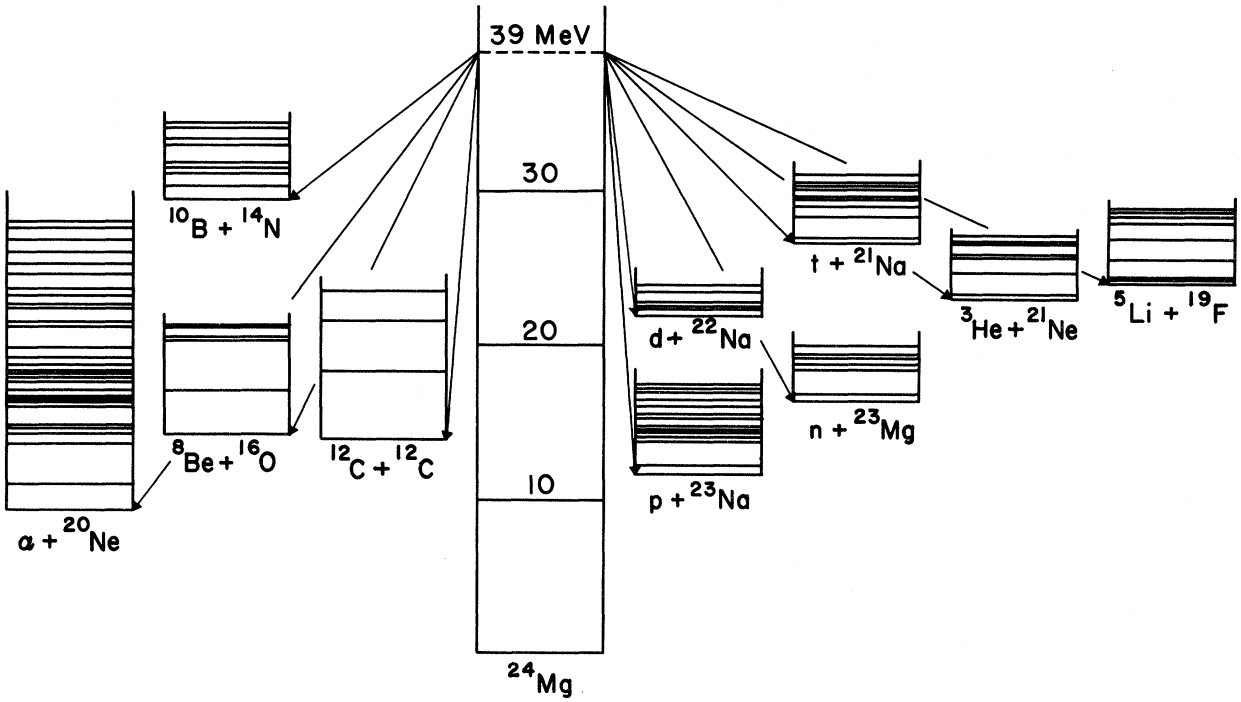

FIG. 11. Energy-level diagram for the ^{24}Mg compound nucleus. The principal open channels, which were used in the Hauser-Feshbach calculations, are shown. The discrete levels used are indicated; level-density equations were used for higher excitations. Note that the $\alpha + ^{20}Ne$ channel has the most favorable Q value. The level at 39 MeV in ^{24}Mg corresponds to an incident ^{12}C energy (lab) of 50 MeV.

VII. HAUSER-FESHBACH STATISTICAL-MODEL CALCULATIONS

In order to make more quantitative estimates concerning the presence of compound-nuclear processes, we have performed detailed Hauser-Feshbach calculations. The details of this procedure, including the computer programs and the equations used, are those of Greenwood *et al.*[3] Whereas one might question the applicability of Hauser-Feshbach theory to the present reaction, previous calculations[1-3] gave excellent agreement with the then available experimental data.

In the compound-nuclear picture the present reaction forms the compound nucleus ^{24}Mg at rather high excitation (30–40 MeV). Once formed, the compound nucleus has a probability for decay into every allowed open channel. The most important channels available are shown in Fig. 11. In a statistical process, the relative cross section to a given channel should depend solely on the probability that a specific particle at a given energy will be able to emerge from the compound nucleus. This probability or optical-model transmission coefficient can be computed. If we then multiply this probability by the probability of forming the compound nucleus, divide by the sum of all other allowed decay probabilities, and weight each quantity by the appropriate statistical factors, we have the total Hauser-Feshbach cross section for a given channel. The results of such a calculation for the present reaction are shown in Fig. 12. The energy dependence of the cross sections for selected levels is shown in Fig. 13. As can be seen, the low-lying levels have a maximum population near $E_{c.m.} \sim 10$ MeV. This may explain why the previous studies[1,2] at this energy found that the reaction mechanism to the ground state and 2^+ level was predominantly compound nuclear.

The optical-model parameters used are given in Table III. Since the sums must extend over states in the continuum, level-density equations were required and the parameters for these are also listed in Table III. All recent compilations of energy levels available in the literature were used to first calculate the discrete contribution to the denominator $G(J)$, and then level-density equations were employed.[21] All transmission coefficients were computed with the optical-model code ABACUS.[22]

Figure 14 shows the denominator calculated at 48 MeV (lab) and shows the contributions from various channels. As can be seen, the $\alpha + ^{20}$Ne channel is the dominant decay mode, especially for higher values of the total angular momentum J. As shown in Fig. 15, the denominator, which is equivalent to the number of open channels, rises very steeply with incident energy.

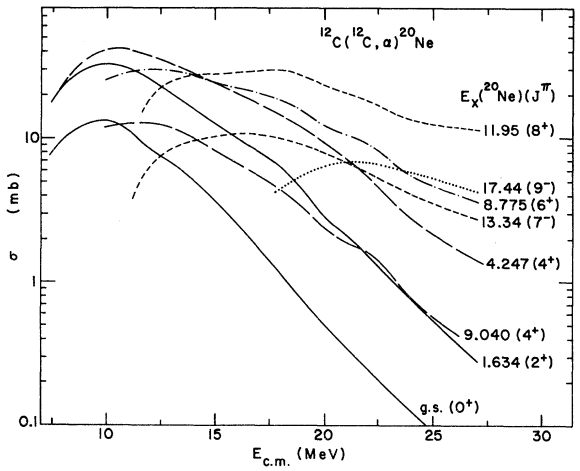

FIG. 12. Total Hauser-Feshbach cross sections as a function of excitation energy for each J^π value in ^{20}Ne at an incident ^{12}C energy of 48 MeV (lab).

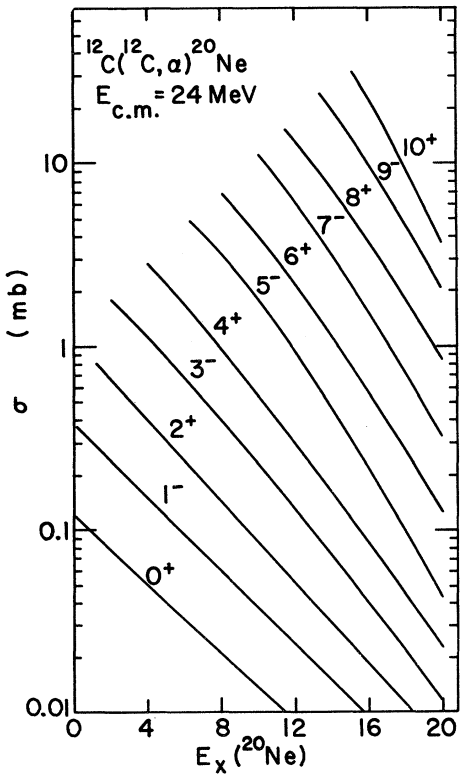

FIG. 13. The energy dependence of the total Hauser-Feshbach cross sections to various levels in ^{20}Ne. Note that the low-lying levels are highest near $E_{c.m.} \approx 10$ MeV, whereas higher excitation, higher-spin levels have a broader energy dependence.

TABLE III. Optical-model and level-density parameters used in Hauser-Feshbach calculations. The level-density notation is that of Ref. 19:

$$\text{Level density} = \rho(E)[2(2\pi)^{1/3}\sigma^3]^{-1}\rho_I \sum_I (2I+1)\exp[-I(I+1)/2\sigma^2],$$

where

$$\rho(E) = [\sqrt{\pi}/12\, a^{1/4}]\, U^{-5/4}\exp[2(aU)^{1/2}], \quad U = E-\Delta, \quad \sigma^2 = 1.44A^{2/3}at/\pi^2, \quad t = [(E-\Delta)/a]^{1/2}.$$

	$\alpha + {}^{20}Ne$	$p + {}^{23}Na$	$n + {}^{23}Mg$	$d + {}^{22}Na$	$^3He + {}^{21}Ne$	$t + {}^{21}Na$	$^5Li + {}^{19}F$	$^8Be + {}^{16}O$ [a]	$^{10}B + {}^{14}N$ [a]	$^{12}C + {}^{12}C$ [a]
a	3.30	3.84	3.84	4.00	4.00	4.00	3.30	b	b	b
Δ	0	2.67	2.67	0	0	0	0	b	b	b
Y [a]	0.20	0.17	0.17	0.17	0.17	0.17	0.17	b	b	b
E_c [c] (MeV)	14.5	5.7	2.9	4.4	4.8	4.5	11.0	17.86	11.95	19.42
V (MeV)	125.3 [d]	47.2 [e]	48 [f]	117 [g]	155 [h]	155 [h]	$7.5 + 0.4E_{c.m.}$		$7.5 + 0.4E_{c.m.}$ [i]	
r_0 (fm)	4.21 [d]	3.56 [e]	3.62 [f]	2.94 [g]	2.98 [h]	2.98 [h]	5.91		$1.35(A_1^{1/3} + A_2^{1/3})$ [i]	
a_0 (fm)	0.54 [d]	0.65 [e]	0.66 [f]	0.86 [g]	0.80 [h]	0.80 [h]	0.65		0.45 [i]	
W (MeV)	30.7 [d]	7.5 [e]	9.6 [f,j]	18.9 [g]	15.0 [h]	15.0 [h]	$0.4 + 0.125E_{c.m.}$		$0.4 + 0.125E_{c.m.}$ [i]	
r_i (fm)	4.34 [d]	3.56 [e]	3.62 [f]	4.46 [g]	4.92 [h]	4.92 [h]	5.91		$1.35(A_1^{1/3} + A_2^{1/3})$ [i]	
a_i (fm)	0.39 [d]	0.65 [e]	0.47 [f]	0.54 [g]	0.60 [h]	0.60 [h]	0.65		0.45 [i]	
R_{Coul} (fm)	4.21 [d]	3.56 [e]		3.64 [g]	3.86 [h]	3.86 [h]	5.91		$1.35(A_1^{1/3} + A_2^{1/3})$ [i]	

[a] $E_{yrast} = YI(I+1)$ = maximum energy for spin I.
[b] Level-density equations not used; discrete levels only.
[c] E_c = energy above which discrete levels were "unknown" and continuum level densities were used.
[d] P. P. Singh, R. E. Malmin, M. High, and D. W. Devins, Phys. Rev. Lett. 23, 1124 (1969).
[e] L. Rosen, Helv. Phys. Acta, Exp. Suppl. 12, 253 (1966).
[f] F. Perey and B. Buck, Nucl. Phys. 32, 353 (1962).
[g] T. J. Yule and W. Haeberli, Nucl. Phys. A117, 1 (1968).
[h] W. P. Alford, D. Cline, H. E. Gove, K. H. Purser, and S. Skorka, Nucl. Phys. A130, 119 (1969).
[i] R. E. Malmin, Ph.D. thesis, Indiana University, 1972 (unpublished).
[j] The imaginary well was of the surface type in this case; all others were the volume type.

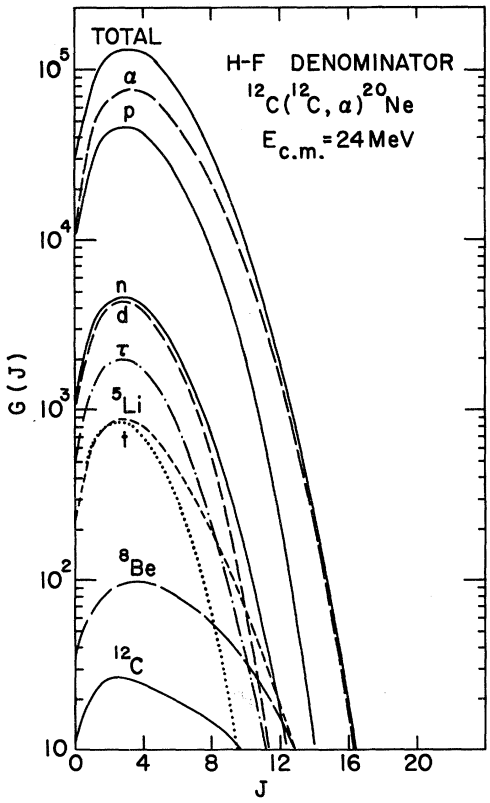

FIG. 14. The total Hauser-Feshbach denominator at E_{lab}=48 MeV. Individual channel contributions are indicated. As can be seen, the $\alpha + ^{20}Ne$ channel dominates, especially at high total angular momentum values.

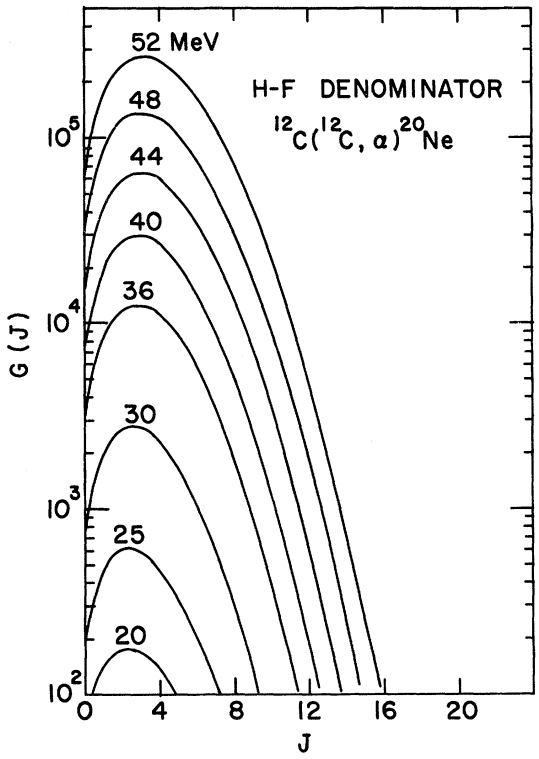

FIG. 15. The total Hauser-Feshbach denominator as a function of total angular momentum J, at various incident energies (lab). The denominator is proportional to the total number of available open channels.

VIII. COMPARISON OF CALCULATIONS WITH EXPERIMENTAL DATA

The computed Hauser-Feshbach cross sections have been compared with both the present data and with that of other studies. Table I and Fig. 3 show a comparison between the measured cross sections averaged over the energy interval $E_{c.m.}$ = 18–25.5 MeV, and the computed cross sections similarly averaged and estimated at $\theta_{c.m.}$ = 7.5° on the assumption of a $1/\sin\theta$ angular distribution. Whereas one might question the validity of the $1/\sin\theta$ assumption at small angles, it appears that our energy-averaged angular distributions are described quite well by this form down to $\theta_{c.m.} \sim 5°$ (see Figs. 6 and 7). The largest errors caused by this assumption would be for the unnatural-parity states. As can be seen, the calculations generally disagree quite badly with the measured values. Any error caused by the $1/\sin\theta$ assumption would be relatively small and certainly could not explain the large discrepancies which we see in Table I. For some of the higher excited states the peaks did not stand out above the continuum at all bombarding energies and for these, which are noted in Table IV, the cross sections were averaged only over those regions where the peaks could be clearly discerned. Thus, for these states, the averages are weighted towards those energies where the peaks are strong and, as such, represent an overestimate of the true average cross sections.

A striking feature of Fig. 3 is that for one $K^\pi = 0^+$ band (7.196, 7.834, 9.04, and 12.16 MeV) the measured cross sections for the first three levels are at least an order of magnitude larger than predicted. The measured cross sections for other levels generally fall within a factor of 5 of the calculated values, except for states with the lowest J^π values. The strong preferential feeding of the 7.196-MeV band is expected if the predominant nuclear configuration is $(sd)^8(1p)^{-4}$, since this configuration can be formed by the direct transfer of an 8-nucleon cluster to ^{12}C. All other bands in ^{20}Ne would require more complicated transfers and hence should be weaker, as is found experimentally. A good example for comparison is the nearby $K^\pi = 0^+$ band (6.722, 7.424, 9.99, and 12.56 MeV) which has predominantly an $(sd)^4$ configura-

TABLE IV. Comparison of experimental and theoretical (Hauser-Feshbach) cross sections by rotational bands. All calculations assumed $W(\theta) \approx 1/\sin\theta$.

J^π	E_x	$\left\langle \frac{d\sigma}{d\omega} \right\rangle_{exp}$	$\left\langle \frac{d\sigma}{d\omega} \right\rangle_{calc}$ No J cut	$\left\langle \frac{d\sigma}{d\omega} \right\rangle_{calc}$ J cut at yrast [a]	Ratio (exp./calc.) No J cut	Ratio (exp./calc.) J cut at yrast
			g.s.—$K^\pi = 0^+$			
0^+	g.s.	0.56	0.16	0.16	3.5	3.5
2^+	1.634	1.53	0.90	0.90	1.7	1.7
4^+	4.247	2.96	2.77	2.2	1.1	1.35
6^+	8.775	2.43	4.0	2.6	0.61	0.94
8^+	11.948	2.75	7.9	3.3	0.35	0.84
			$K^\pi = 0^+$			
0^+	6.722	0.21	0.031	0.031	6.8	6.8
2^+	7.424	0.36	0.185	0.185	2.0	2.0
4^+	9.99	1.16	0.56	0.56	2.1	2.1
(6^+)	(12.56)	···	1.5	1.3		
			$K^\pi = 0^+$			
0^+	7.196	1.00 [b]	0.028	0.028	36 [b]	36 [b]
2^+	7.834	1.92	0.162	0.162	11.8	11.8
4^+	9.040	8.21	0.78	0.76	10.5	10.8
6^+	12.16	3.59	1.6	1.35	2.2	2.7
(8^+)	16.76	≈1.6	1.25	0.97	≈1.3	≈1.7
			$K^\pi = 2^-$			
2^-	4.968	0.24	0.14	0.14	1.7	1.7
3^-	5.622	0.69	0.84	0.83	0.82	0.83
4^-	7.006	0.37	0.57	0.56	0.65	0.66
5^-	8.447	2.04	2.2	1.8	0.93	1.1
6^-	10.609	···	1.2	1.1	(<1) [b]	···
7^-	13.34	3.65	2.5	1.7	1.45	2.2
8^-	15.62	···	0.9		(<1) [b]	···
9^-	17.44	3.57	2.3	1.4	1.5	2.5
			$K^\pi = 1^-$			
1^-	5.785	0.74	0.11	0.11	6.7	6.7
3^-	7.166	W [b]	0.53	0.53	(<1) [b]	···
5^-	10.257	···	1.33	1.33		
7^-	(15.360)	···				
			Unplaced levels			
2^+	9.489	0.49	0.10	0.10	4.9	4.9
$(3^-, 0^+)$	12.40	1.39 [c]				
$(2^-, 4^+)$	13.07	1.34				
(6^+)	13.95	4.65	0.80	0.80	5.8	5.8
(6^+)	14.35	2.85 [c]	0.68	0.68	4.2 [c]	4.2 [c]
	14.79	≈1.6 [c]				
(6^+) or (9^-)	15.20	1.97	0.40		4.9	
	15.40	≈1.4 [c]				
$(5^-, 8^+)$	15.93	3.87				
$(6^+, 7^-)$	18.15	1.29 [c]				
	18.50	2.54 [c]				

[a] Assumed $J_{max} = 14$ at all but 36 MeV, where $J_{max} = 12$ (see text).
[b] Level not resolved.
[c] Average not over entire energy interval.

tion. As seen in Table I, the average experimental cross sections are about a factor of 5 to 7 lower than for the nearby $K^\pi = 0^+$ band, even though corresponding states have similar excitation energies. The Hauser-Feshbach calculations predict that the two bands should be about equally excited. Convincing evidence is therefore present that at least for the 8p-4h band the reaction does not proceed solely by a statistical compound-nuclear process.

There are other noteworthy trends in the comparison between measured and calculated compound-nuclear cross sections. In Table IV the ratio of the measured to calculated cross section is listed by rotational bands. It can be seen that for the ground-state band this ratio decreases sharply as a function of spin, falling from 3.5 for the ground state to 0.35 for the 11.95-MeV (8^+) state. A similar trend is also evident for the other two $K^\pi = 0^+$ bands. The failure to correctly predict the spin dependence of the cross sections may be due in part to the neglect of any cutoff on the allowed spins of states in the compound nucleus. For high-spin states at low excitation energies in ^{20}Ne, it is evident from the calculations that most of the cross section comes from high-spin states in ^{24}Mg. This may be entirely unrealistic since a reasonable yrast cutoff in ^{24}Mg of $E_{\text{c.m.}} = 0.16I(I+1)$ (obtained from the energies within the ground-state band) would predict no states with $I = 16$ below 43.5 MeV in ^{24}Mg (E_{lab} ^{12}C ≈ 59 MeV) and no states with $I = 14$ below 33.6 MeV (E_{lab} ^{12}C ≈ 39 MeV). Calculations were also performed using this yrast spin cutoff in ^{24}Mg, the results of which are shown in Table IV. Introducing the cutoff had the effect of lowering the calculated cross sections for the higher-spin states of the ground-state band, thereby improving the agreement with experiment. The effects on the calculations for populating the higher bands were somewhat smaller and there was no apparent improvement in the agreement with experiment; in fact, for the 2^- band the agreement is noticeably worse. Thus, the net result of introducing the cutoff was to improve the fit to the ground-state band, leaving only the ground state itself in serious disagreement. The calculated cross sections to all other states in ^{20}Ne are changed only slightly, with the largest effect being about a 20% reduction in the calculated cross sections to the 7^- and 9^- members of the $K^\pi = 2^-$ band, thereby making the fit to this band slightly worse than before.

The results given in Table IV are remarkably good for the $K^\pi = 2^-$ band starting at 4.968 MeV. This band contains both natural- and unnatural-parity states, and the unnatural-parity states cannot be excited by the direct transfer of a ^{8}Be cluster in its ground state since ^{12}C and ^{8}Be both are $J^\pi = 0^+$. On the other hand, the feeding of unnatural-parity states through the compound nucleus is uninhibited. It is thus interesting to note that the measured cross sections agree well with the calculated compound-nuclear values for this band for both natural- and unnatural-parity states. This would also appear to validate the assumption of a $1/\sin\theta$ average angular dependence since we would expect this assumption to be worse for the unnatural-parity states. Furthermore, for this band there is no evidence that the lower-spin states have a larger ratio of measured to calculated cross sections (Table IV) than do high-spin states, as seen for the other three bands. Hence, it would appear from the Hauser-Feshbach calculations that the measured cross sections for this band are consistent with a compound-nuclear process. However, the Ericson analysis of the excitation functions presented above indicates the presence of large direct components—e.g., $R(\Gamma, 0) = 0.27$ and hence $Y_d = 0.68$–0.85 for the 4.968-MeV 2^- level. The discrepancy between the two determinations of the ratio of direct to compound components may not be as severe as first appears since, on the one hand, the Hauser-Feshbach calculations are sufficiently inaccurate so as to leave room for a sizable direct component while, on the other hand, the extraction of the direct part in the Ericson analysis can also have a large error. In order to compare these two independent determinations of the size of the direct component, we have calculated Y_d from the difference between the experimental cross sections and the Hauser-Feshbach calculations. The results are given in Table I. In spite of the large error inherent in this method, we find that the two independent determinations of Y_d are generally consistent. The largest differences are seen for the $K^\pi = 2^-$ band and part of the difference could be ascribed to our $1/\sin\theta$ assumption, especially for the unnatural-parity states. Differences seen for other levels could be partly explained if we used the Hauser-Feshbach results based on the J cutoff at the yrast level, as given in Table IV. However, it must be admitted that when all of the levels in ^{20}Ne are considered, the Ericson analysis indicates a much more constant fraction of direct component from level to level than can be inferred from other considerations. At present, we can only ascribe this difficulty to quantitative inadequacies in the Ericson methods.

The present Hauser-Feshbach calculations are also compared to the previous data and to calculations of Borggreen *et al.*[1] and Vogt *et al.*[2] in Table V. As can be seen, the present calculations agree well with those of Borggreen *et al.*, but predict somewhat lower cross sections than do those of Vogt *et al.* Such differences are not surprising

TABLE V. Comparison of theoretical Hauser-Feshbach cross sections (σ_T^{HF}) with experimental data (σ_T^{exp}) of Refs. 1 and 2.

E_x (MeV)	J^π	σ_T^{exp} (mb)	σ_T^{HF} [a] (mb)	σ_T^{HF} (mb) b	c
0	0^+	20 [b]	10.5	10.5	16.0
		19.2 [c]			
1.634	2^+	64 [b]	27.3	28.0	39.3
		63 [c]			
Ratio:	$2^+/0^+$	3.2	2.6	2.7	2.5

[a] Present work—calculated for $E_{c.m.}$=10–12.5 MeV.
[b] Reference 1, $E_{c.m.}$=10.1–12.8 MeV.
[c] Reference 2, $E_{c.m.}$=10.15–12.8 MeV.

considering the large number of differences in the parameters that were used. It is felt that the present calculations are more accurate since many more open channels have been used and the level energies, optical-model parameters, and level-density parameters are from more recent data. We note that whereas the calculations agree fairly well, they are lower than the measured cross sections by about a factor of 2. It is unlikely that that difference between the calculated and measured cross sections in the low-energy region can be attributed to a direct component since a direct component as large as that extracted from our data, when extrapolated to $E_{c.m.}$=10 MeV, would be only a very small fraction of the measured cross section at that energy. Furthermore, previous analysis[1,2] of the data in this energy region found the reaction to be compatible with going 100% through the compound nucleus. It is more likely that this discrepancy again indicates the degree to which the absolute magnitudes of the calculated compound-nuclear cross sections are uncertain. However, the calculated relative cross sections may be more reliable. The measured ratio of the 2^+ to 0^+ cross sections is about 3.2, whereas the calculations predict about 2.6.

CONCLUSIONS

Both compound nucleus and direct reaction appear to contribute to the $^{12}C(^{12}C, \alpha)^{20}Ne$ reaction in the energy region we have studied. The strong fluctuations in the yield curves require the presence of the narrow compound-nucleus levels, while the selective feeding of certain states indicates the presence of a strong direct component. The selectivity of the reaction stands out strongly when the feeding of states in the intertwined $K=0^+$ bands starting at 6.72 and 7.20 MeV are compared. Further support for the contention that the reaction is largely direct comes from statistical (i.e., Hauser-Feshbach) calculations which predict cross sections that, at least for the low-spin states, are substantially smaller than those that are observed. Analyzing the data in terms of Ericson fluctuations leads to the conclusion that both direct and compound-nucleus contributions are present with the direct dominant. However, the Ericson analysis fails to find larger direct components for those states for which the cross section is especially large compared to the Hauser-Feshbach calculations.

Statistical analysis demonstrates the existence of a 500-keV-wide anomaly at $E_{c.m.}$=19.2 MeV which is near to the energy of a resonance reported in the $^{12}C(^{12}C, p)^{23}Na$ reaction. It is concluded that the resonance in the proton channel is taking flux from the α channel.

Previously proposed band structure in ^{20}Ne has been confirmed and, to some degrees, extended. The 4^+ and 6^+ states of the two 0^+ bands whose heads are at about 7 MeV are definitely placed. Higher members of other bands are assigned, with varying degrees of certainty. The pattern of average cross sections agrees with proposed configurations for the various bands and indicates a substantial amount of direct 8-nucleon transfer.

Over all, we conclude that a study of the $^{12}C(^{12}C, \alpha)^{20}Ne$ reaction is an effective means of studying both the reaction mechanism and the nuclear structure of ^{20}Ne. In doing such a study it is necessary that an energy region large compared to the width of the individual compound-nucleus levels be covered. Encouragement can be gained from the present work that the $(^{12}C, \alpha)$ and similar reactions can be utilized to study clustering in nuclei.

*Work supported by the U. S. Atomic Energy Commission and the National Science Foundation.

[1] J. Borggreen, B. Elbek, and R. B. Leachman, K. Dan. Vidensk. Selsk. Mat.—Fys. Medd. 34, 9 (1964); J. P. Bondorf and R. B. Leachman, *ibid.* 34, 10 (1965).
[2] E. W. Vogt, D. McPherson, J. A. Keuhner, and E. Almqvist, Phys. Rev. 136, B84, B99 (1964).
[3] L. R. Greenwood, K. Katori, R. E. Malmin, T. H. Braid, J. C. Stoltzfus, and R. H. Siemssen, Phys. Rev. C 6, 2112 (1972).
[4] M. L. Halbert, F. E. Durham, and A. Van der Woude, Phys. Rev. 162, 899, 919 (1967).
[5] R. Middleton, J. D. Garrett, and H. T. Fortune, Phys. Rev. Lett. 27, 950 (1971).

[6]Y. Akiyama, A. Ariman, and T. Sebe, Nucl. Phys. A138, 273 (1969).
[7]K. Van Bibber, E. R. Cosman, A. Sperduto, T. M. Cormier, and T. N. Chin, Phys. Rev. Lett. 32, 687 (1974).
[8]L. R. Greenwood, Argonne Physics Division Informal Report No. PHY-1970B (unpublished).
[9]F. Ajzenberg-Selove, Nucl. Phys. A190, 1 (1972).
[10]R. E. Malmin, R. H. Siemssen, D. A. Sink, and P. P. Singh, Phys. Rev. Lett. 28, 1590 (1972).
[11]T. Ericson, Ann. Phys. (N.Y.) 23, 390 (1963).
[12]D. M. Brink, Nucl. Phys. 54, 575 (1964).
[13]For example see, J. R. Erskine, W. Henning, D. G. Kovar, and L. R. Greenwood, Phys. Rev. Lett. 34, 680 (1975).
[14]R. M. DeVries, Phys. Rev. C 8, 951 (1973).
[15]T. D. Thomas, Annu. Rev. Nucl. Sci. 18, 343 (1968).
[16]G. M. Temmer, Phys. Rev. Lett. 12, 330 (1964).
[17]R. C. Bearse, L. Meyer-Schützmeister, and R. E. Segel, Nucl. Phys. A116, 682 (1968).
[18]D. Shapira, R. G. Stokstad, and D. A. Bromley, Phys. Rev. C 10, 1063 (1974).
[19]L. R. Greenwood, H. T. Fortune, R. E. Segel, and J. R. Erskine, Phys. Rev. C 10, 1211 (1974).
[20]H. T. Fortune, L. R. Greenwood, R. E. Segel, K. Raghunathan, and J. R. Erskine, unpublished.
[21]U. Facchini and E. Saetta-Menichella, Energia Nucl. 15, 54 (1968).
[22]E. H. Auerbach (private communication).